Eighteenth Symposium (International) on Combustion The Combustion Institute, 1981

MONTE CARLO CALCULATIONS OF PREMIXED TURBULENT FLAMES

S. B. POPE
Department of Mechanical Engineering
Massachusetts Institute of Technology
Cambridge, Massachusetts 02139

Calculations of turbulent premixed propane/air flames are presented and compared with the experimental data of Robinson.[1] The flames are stabilized behind a perforated plate in a constant diameter tube and the effects of flame-holder solidity and equivalence ratio are studied. Good agreement is found between the measured and calculated concentrations of CO and NO.

The calculations are based on the transport equation for the joint probability density function (*pdf*) of three species—C_3H_8, CO and NO. This equation[2] takes proper account of turbulent transport and mixing while allowing the chemical kinetics to be treated without approximation. Since the joint *pdf* is a function of five variables (three species, one space dimension, and time) its solution by finite-difference techniques is not feasible. However, the equation is readily solved by a Monte Carlo method.[3] In general the calculated concentrations of CO and NO are in good agreement with the measurements although, for the weakest mixture, the reaction rates appear to be underestimated.

The calculations clearly demonstrate that the Monte Carlo method can be used to solve the joint *pdf* equation for inhomogeneous turbulent flows.

Introduction

In this paper, calculations of local species concentrations in turbulent premixed propane/air flames are presented and compared with the data of Robinson.[1] The calculations are based on the solution of the transport equation for the joint probability density function (*pdf*) of three species —C_3H_8, CO and NO. This equation[2] has the virtue of taking due account of the turbulence while admitting finite-rate chemical kinetics. In fact, the effects of reaction appear in closed form in the *pdf* equation irrespective of the complexity and non-linearity of the reaction scheme. The joint *pdf* equation is solved by a Monte Carlo method[3] and the resulting calculations (including CO and NO concentrations) are in good agreement with the data.

The main difficulty in the theoretical treatment of turbulent flames is the highly non-linear coupling between the turbulence and the reaction. For diffusion flames this problem can usually be circumvented by assuming that chemical equilibrium prevails; then standard turbulence modelling techniques can be used to obtain reasonably accurate calculations.[4] In general, however, moment formulations (such as turbulence models) are incapable of dealing with the non-linear coupling between the turbulence and the reaction. Consequently, for premixed flames, especially when finite-rate reactions are of interest, other methods are required.

The *pdf* approach is seen by several workers[2,5,6,7,8] to be a promising way to treat turbulent reaction. This is because the joint *pdf* of the chemical and thermodynamic properties contains all the statistical information required to determine mean reaction rates. Further, in the *pdf* transport equation, the term pertaining to reaction appears in closed form: it requires no modelling assumptions. A major difficulty appeared to be that the *pdf* equation was prohibitively difficult to solve for all but the simplest of cases. Finite-difference methods have difficulty in coping with the large dimensionality of the *pdf*'s and the integro-differential nature of the equations. However, these difficulties are not inherent to all methods: a Monte Carlo method has been devised[3] which makes possible the solution of the *pdf* equation for the general case.

The objectives of the work reported here are to use the Monte Carlo method to solve the joint *pdf* equation for turbulent premixed propane/air flames,

and to compare the results with data.[1] The Monte Carlo calculations demonstrate the use of the method, and the comparison of calculations with measurements allows the accuracy of the modelled *pdf* equation to be assessed.

The flames studied by Robinson[1] were stabilized behind a perforated plate in a 4″ diameter tube. Three different plates and three different equivalence ratios were used, giving nine possible combinations. The three plates had different numbers of 1/4″ diameter holes, to produce solidity ratios $s = 0.742$, $s = 0.815$ and $s = 0.892$. (The solidity ratio is defined as the blocked area divided by the total area.) The homogeneous propane/air mixture was supplied at a temperature of 590 K, a pressure of 5×10^5 Pa, and an equivalence ratio ϕ of 0.635, 0.725 or 0.825. For each of the nine flames, concentrations of CO and NO were measured at axial locations up to 15″ downstream of the perforated-plate flame holder. Maximum temperatures and flow velocities in the flames were of order 1900 K and 100 m/s.

The equations solved and the method of solution are outlined in the next section: the results of the calculations are then compared with Robinson's data. Conclusions are drawn in the final section.

Theory

The joint *pdf* $p(\underline{\psi}; \underline{x}, t)$ is a function of space and time $(\underline{x}, t)$, and composition $\underline{\psi}$. The flow considered is three-dimensional and at least twelve species are involved. Hence, if no simplifications were made, $p(\underline{\psi}; \underline{x}, t)$ would be a function of sixteen variables. Of course, simplifications are possible. After the *pdf* equation is presented in the first sub-section, simplifications are made to reduce the number of independent reactants to three—namely, C_3H_8, CO and NO. In the third sub-section a flow and turbulence model is described which reduces the number of spatial variables to one—ξ. The final sub-section outlines the Monte Carlo method for solving the transport equation for $p(m_{C_3H_8}, m_{CO}, m_{NO}; \xi, t)$.

The Joint *pdf* Equation

The form of the *pdf* equation used is that described by Pope.[3] The dependent variable is $\tilde{p}(\underline{\psi}; \underline{x}, t)$ which is the density-weighted joint *pdf* of a set of scalars $\underline{\phi}$ ($\underline{\psi}$ is the compostion space corresponding to $\underline{\phi}$). In the present study $\underline{\phi}$ comprises the three mass fractions $m_{C_3H_8}$, m_{CO} and m_{NO}. Any density-weighted average can be determined from $\tilde{p}$ by, for example,

$$\tilde{Q} \equiv \langle \rho Q \rangle / \langle \rho \rangle = \int \tilde{p}(\underline{\psi}) Q(\underline{\psi})\, d\underline{\psi}, \qquad (1)$$

where Q is any function of ϕ, ρ is the density and integration is over the whole of $\underline{\psi}$-space.

A transport equation for $\tilde{p}(\underline{\psi})$ can be obtained from the conservation equations for $\underline{\phi}$.[2,3] If the turbulent transport is modelled by simple gradient diffusion (with the turbulent diffusion coefficient being $\Gamma_T(\underline{x}, t)$), the equation for $\tilde{p}(\underline{\psi})$ is

$$\frac{\partial \tilde{p}}{\partial t}(\underline{\psi}) + \tilde{U}_i \frac{\partial \tilde{p}}{\partial x_i}(\underline{\psi}) + \frac{\partial}{\partial \psi_\alpha}(\tilde{p}(\underline{\psi}) S_\alpha(\underline{\psi})) = \frac{1}{\langle \rho \rangle} \frac{\partial}{\partial x_i} \Gamma_T \frac{\partial \tilde{p}}{\partial x_i}(\underline{\psi}) + E(\underline{\psi}; \underline{x}, t). \qquad (2)$$

Summation is over repeated indices (i and α), $S_\alpha(\underline{\phi})$ is the rate of change of ϕ_α due to reaction, and $E(\underline{\psi}; \underline{x}, t)$ represents the effect of molecular mixing. The terms on the left-hand side are exact whereas those on the right are modelled or (in the case of E) need to be modelled. The two leading terms represent the rate of change of $\tilde{p}(\underline{\psi})$ along a density-weighted streamline; the third term represents the transport of $\tilde{p}(\underline{\psi})$ in composition space due to reaction. It is noteworthy that, in this formulation, reaction—however complicated the scheme—can be treated without approximation.

Curl's model[9] is used for the mixing term:

$$E(\underline{\psi}; \underline{x}, t) = 2^\sigma \omega \int \tilde{p}(\underline{\psi} + \underline{\psi}')\, \tilde{p}(\underline{\psi} - \underline{\psi}')\, d\underline{\psi}' - \omega \tilde{p}(\underline{\psi}) \qquad (3)$$

where $\omega(\underline{x}, t)$ is the appropriate turbulent frequency and σ is the dimensionality of $\underline{\psi}$-space (here $\sigma = 3$). A more complete discussion of the modelling is given by Pope.[2]

The turbulent diffusion coefficient Γ_T and frequency ω are related to the k-ϵ turbulence model[10] parameters by

$$\Gamma_T = C_\mu \langle \rho \rangle k^2 / (\epsilon \sigma_\phi), \qquad (4)$$

and

$$\omega = 2 C_\phi \epsilon / k, \qquad (5)$$

where the values of the constants C_μ, σ_ϕ and C_ϕ are 0.09, 0.7 and 2.0, respectively.

Reaction Scheme

The computational effort required to solve the joint *pdf* equation depends crucially on the complexity of the reaction scheme. Consequently, although twelve reactions involving as many species are considered, assumptions are made to reduce the number of independent reactants to three.

The processes of main interest are the burn out

of CO and the formation on NO. Consequently the initial breakdown of C_3H_8 is not treated in any detail. It is assumed that, as soon as the temperature of the fuel/air mixture rises infinitesimally above the inlet temperature, it burns to form CO and an equilibrium mixture of H, H_2, H_2O, O, OH and O_2.

The subsequent oxidation of CO is modelled using a partial equilibrium assumption similar to that of Morr and Heywood.[11] The oxidation of CO proceeds at a finite rate by the reaction

$$CO + OH \rightleftharpoons H + CO_2. \qquad \text{(i)}$$

The two body reactions are very rapid compared with flow or turbulent time scales and consequently are assumed to be in equilibrium. These reactions conserve the number of moles. The relatively slow three-body reactions are used to determine the rate of change of the number of moles. Starting from the initial condition of CO and equilibrium O, H, etc., appropriate to the given equivalence ratio, the rate of change of CO is determined by reaction (i), and the rate of change of the number of moles is determined from the three-body reactions: the composition is then determined by the equilibrium of two-body reactions. Since the mass fraction of CO, m_{CO}, decreases monotonically with time, a unique relationship is obtained between each species mass fraction and m_{CO}. Thus the properties of the C—O—H system are obtained from the single variable m_{CO}.

The formation of NO is described by the extended Zeldovich mechanism with the steady-state assumption for the N-atom concentration.

Thus, all the properties and their rates of change can be determined from the mass fractions $m_{C_3H_8}$, m_{CO} and m_{NO}: consequently a complete statistical description is provided by the joint *pdf* $p(m_{C_3H_8}, m_{CO}, m_{NO}; x,t)$.

Reaction rates were obtained from Jensen and Jones[12] and thermodynamic data from Gordon and McBride.[13]

Turbulence and Flow Model

The flow behind a perforated plate is three-dimensional. Jets issue from the holes in the plate, and in between the jets there are turbulent recirculation zones. Further downstream, the jets merge and eventually the mean velocity becomes uniform. Rather than affording the extravagance of a three-dimensional calculation, it was decided to reduce the problem to one dimension by considering area-averaged quantities. Therefore, only the axial independent variable is retained. The remainder of this sub-section describes the assumptions made in reducing the problem to one dimension.

The flow is sketched in Fig. 1. The axial distance downstream of the plate x_1 is normalized by the diameter d of the holes to form the new independent variable

$$\xi \equiv x_1/d. \qquad (6)$$

As is illustrated in the figure, the flow is considered in three regions. Region I comprises the potential cores of the jets: these are assumed to be conical and, from the data assembled by Hill,[14] their length is taken to be $l_c = 7.5\ d$. Region II comprises the turbulent flow outside the potential cores ($0 < \xi \leq 7.5$) and Region III extends downstream to the end of the solution domain ($7.5 < \xi \leq 60$).

Region I (the potential cores) is a region of uniform properties. The gas composition is the same as the unburnt mixture upstream, and the uniform velocity U_1 is determined by mass conservation from the upstream velocity U_0:

$$U_1 = U_0/(1 - s^*). \qquad (7)$$

s^* is the effective solidity ratio which accounts for the decreased area due to the vena contracta. The measured pressure drop across the plates shows that the effective area ratio is given by

$$(1 - s^*) = 0.86(1 - s). \qquad (8)$$

In Regions II and III the velocity $\underline{U}(x,t)$ can be decomposed into the density-weighted mean $\tilde{U}(x,t)$ and fluctuations $u''(x,t)$:

$$\underline{U}(x,t) = \tilde{U}(x,t) + u''(x,t). \qquad (9)$$

The mean can be further decomposed into its area average $\bar{U}(x_1,t)$ and departures from it $\underline{U}^*(x,t)$:

$$\tilde{U}(x,t) = \bar{U}(x_1,t) + \underline{U}^*(x,t). \qquad (10)$$

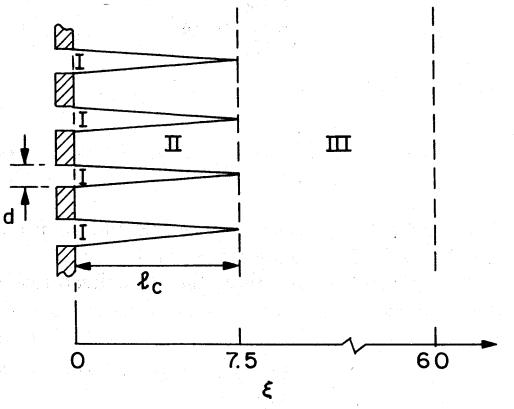

FIG. 1. Sketch of the flow behind a perforated plate.

It may be noted that $\bar{U}$ is only a function of x_1 (or ξ) and that its only component is in the x_1-direction. It is emphasized that in Region II the average is over that region alone, not over Regions I and II. In the present model, the reduction to the single spatial variable ξ is achieved by treating the departures from uniformity $\underline{U}^*(\underline{x},t)$ as if they were turbulence. Thus, for example, the "turbulent" kinetic energy $k(\xi)$ represents both turbulence and the energy associated with $\underline{U}^*(\underline{x},t)$.

The area-averaged density-weighted velocity in Region III is determined by mass conservation:

$$\bar{\rho}(\xi)\bar{U}(\xi) = \rho_0 U_0, \tag{11}$$

where $\bar{\rho}(\xi)$ and ρ_0 are the area-averaged and upstream densities. In Region II the result is

$$\bar{\rho}(\xi)\bar{U}(\xi) = \rho_0 U_0/(1 + s^*[7.5/\xi - 1]). \tag{12}$$

In Region II it is assumed that the turbulent kinetic energy $k = k_2$ and its rate of dissipation $\epsilon = \epsilon_2$ are uniform, and that ϵ_2 scales with k_2 and d,

$$\epsilon_2 = \beta k_2^{3/2}/d, \tag{13}$$

where β is a constant to be determined. Then, for a constant-density (inert) flow, k_2 can be determined from a kinetic energy balance over Regions I and II:

$$k_2 + 5\beta\left(1 + \frac{1}{2}s^*\right)k_2^{3/2} = \frac{1}{2}\left(\frac{s^*}{1 - s^*}\right)^2. \tag{14}$$

Thus, once β has been determined, equation (14) can be solved for k_2, and then ϵ_2 can be obtained from equation (13). While this analysis is for constant-density flows, it is assumed that the same result holds in general.

In Region III k and ϵ decay according to the k-ϵ model[10] (neglecting axial diffusion):

$$\frac{\bar{U}}{d}\frac{dk}{d\xi} = -\epsilon \tag{15}$$

and

$$\frac{\bar{U}}{d}\frac{d\epsilon}{d\xi} = -C_{\epsilon_2}\epsilon^2/k. \tag{16}$$

The constant C_{ϵ_2} takes the value 1.90 and the initial conditions at $\xi = 7.5$ are $k = k_2$ and $\epsilon = \epsilon_2$.

For constant-density flow, the normalized turbulence intensity

$$u' \equiv \left(\frac{2}{3}k\right)^{1/2}/U_0 \tag{17}$$

obtained from equations (13) – (16) is plotted against ξ on Fig. 2. In the initial region ($\xi < 30$) there is a qualitative difference between the calculations and Robinson's experimental data. The data show an initial rise in u' as the turbulence gains energy from the decaying jets. Subsequently the turbulence decays. In the model, k represents both the turbulence energy and the energy of the jets. Consequently, only after the velocity profiles become uniform ($\xi > 30$) is it reasonable to expect the calculated and measured values of u' to agree. The value of $\beta = 0.25$ was selected in order to obtain agreement over the interval $30 < \xi < 60$. It may be seen from Fig. 2 that this simple model appears to account correctly for the influence of solidity ratio upon the turbulence intensity.

In the potential cores (Region I) the joint *pdf* $\tilde{p}(\underline{\psi};\underline{x},t)$ is uniform

$$\tilde{p}(\underline{\psi};\underline{x},t) = p_1(\underline{\psi}) = \delta(\underline{\psi} - \underline{\phi}_0), \tag{18}$$

where $\underline{\phi}_0$ is the composition of the unburnt mixture. ($\underline{\psi} = \psi_1, \psi_2, \psi_3$, it may be recalled, is the composition space corresponding to $\underline{\phi} = m_{C_3H_8}, m_{CO}, m_{NO}$). In Regions II and III an equation for the area-averaged, density-weighted joint *pdf* $\bar{p}(\underline{\psi};\xi,t)$ is obtained by taking the area average of equation (2). The result is

$$\frac{\partial \bar{p}}{\partial t} + \frac{\bar{U}}{d}\frac{\partial \bar{p}}{\partial \xi} + f(\xi)(\bar{p} - p_1)/\bar{\rho} + \frac{\partial}{\partial \psi_\alpha}(\bar{p}(\underline{\psi})S_\alpha(\underline{\psi})) = (\bar{\rho}\, d^2)^{-1}\frac{\partial}{\partial \xi}\Gamma_T\frac{\partial \bar{p}}{\partial \xi} + E(\underline{\psi};\xi,t). \tag{19}$$

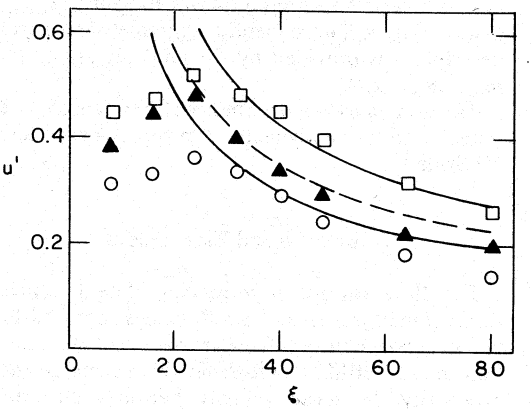

FIG. 2. Turbulence intensity against axial distance.

□ $s = 0.892$
▲ $s = 0.815$
○ $s = 0.742$
} data of Robinson[1]
—calculations

Except for the addition of the third term, the form of the equation is unchanged. The additional term represents convection from Region I into Region II. $f(\xi)$ is the mass flux per unit length across the interfaces between the two regions,

$$f(\xi) = \frac{8}{225}\rho_o U_o(7.5-\xi)/d, \quad \xi \le 7.5$$

$$f(\xi) = 0, \qquad \xi > 7.5. \tag{20}$$

Monte Carlo Method

A complete set of equations for $\bar{p}(m_{C_3H_8}, m_{CO}, m_{NO}; \xi, t)$ has now been obtained, the principal equation being the joint *pdf* equation, Eq. 19. The functions appearing in this equation are the velocity $\bar{U}(\xi,t)$ (Eqs. 11-12), the mass flux per unit length $f(\xi)$ (Eq. 20), the diffusion coefficient $\Gamma_T(\xi,t)$ (Eq. 4), the mixing term $E(\psi; \xi, t)$ (Eq. 3), and the rates of change $S_\alpha(\psi)$ which are obtained from the reaction scheme. The turbulence quantities $k(\xi,t)$ and $\epsilon(\xi,t)$ are obtained from equations 13-16. The only connection between these functions—$\bar{U}$, Γ_T, k and ϵ—and the joint *pdf* is through the density $\bar{\rho}(\xi,t)$ which is determined from the relation

$$1/\bar{\rho}(\xi,t) = \int \bar{p}(\underline{\psi}; \xi, t)/\rho(\underline{\psi})\, d\underline{\psi}. \tag{21}$$

The complete set of equations contains standard turbulence model constants and the constant $\beta = 0.25$. It may be noted, however, that there are no adjustable parameters.

All Robinson's measurements are time means, taken after the steady state has been reached. The calculations are made in the same way, with the joint *pdf* equation being solved by a Monte Carlo method, and the results being obtained after the steady state has been reached. (In fact, the equations for $\bar{U}$, k and ϵ are only valid in the steady state.)

The Monte Carlo method used to solve the general *pdf* equation is described in Ref. 3 where a proof of convergence and error estimates are obtained. A brief description of the method applied to the present equation, Eq. 19, is given here, but the reader is referred to Ref. 3 for more details and an analysis of the scheme.

Finite-difference nodes are located on the interval $0 \le \xi \le 60$, the j^{th} being at ξ_j. At each node there is an ensemble of N elements and at time t the n^{th} element has the properties

$$\underline{\phi}^{(n)}(\xi_j,t) = m^{(n)}_{C_3H_8}(\xi_j,t),\ m^{(n)}_{CO}(\xi_j,t),\ m^{(n)}_{NO}(\xi_j,t). \tag{22}$$

The ensemble average of any function $Q(\underline{\phi})$ is then defined by

$$\hat{Q}(\xi_j,t) \equiv \frac{1}{N}\sum_{n=1}^{N} Q(\underline{\phi}^{(n)}(\xi_j,t)). \tag{23}$$

In the Monte Carlo simulation, in order to advance time from t to $t + \Delta t$, elements are moved from node to node and their values are changed in a prescribed manner. The simulation is constructed so that (as N tends to infinity and the grid spacing tends to zero) the ensemble average $\hat{Q}(\xi_j,t)$ converges to the density-weighted area average $\bar{Q}(\xi_j,t)$,

$$\bar{Q}(\xi_j,t) = \int \bar{p}(\underline{\psi}; \xi_j, t)\, Q(\underline{\psi})\, d\underline{\psi}, \tag{24}$$

where $\bar{p}(\psi; \xi_j, t)$ is the solution to Eq. 19.

The joint *pdf* equation, Eq. 19, shows that $\bar{p}$ changes in time due to five processes: convection, convection from Region I, reaction, diffusion and mixing. In the Monte Carlo method, these processes are simulated sequentially to advance time from t to $t + \Delta t$. For the ensemble at ξ_j the simulations are as follows:

Convection: n_c elements selected at random are replaced by n_c elements selected from the upstream ensemble. The number n_c is

$$n_c = \Delta t N \bar{U}(\xi_j) d^{-1}/(\xi_j - \xi_{j-1}). \tag{25}$$

Convection from Region I: n_1 elements selected at random are replaced by elements with the composition of the unburnt mixture $\underline{\phi}_o$. The number replaced is

$$n_1 = \Delta t N f(\xi_j)/\bar{\rho}(\xi_j). \tag{26}$$

Diffusion: n_{d+} and n_{d-} elements are selected at random from the ensembles at ξ_{j+1} and ξ_{j-1} respectively. They are used to replace $n_{d+} + n_{d-}$ elements selected at random from the ensemble at ξ_j. The numbers n_{d+} and n_{d-} are

$$n_{d\pm} = \Delta t N \Gamma_T\left(\frac{1}{2}(\xi_j + \xi_{j\pm1})\right) \cdot [\bar{\rho}(\xi_j) d^2 (\xi_{j+1} - \xi_{j-1})|\xi_{j\pm1} - \xi_j|]^{-1}. \tag{27}$$

Mixing: The following operation is repeated n_m times, where

$$n_m = \frac{1}{2}\Delta t N \omega(\xi_j). \tag{28}$$

Two elements, denoted by n and m, are selected at random. Their properties $\underline{\phi}^{(n)}(\xi_j)$ and $\underline{\phi}^{(m)}(\xi_j)$ are then replaced by their average value $\underline{\phi}^{(mix)}$

$$\underline{\phi}^{(mix)} = \frac{1}{2}[\underline{\phi}^{(n)}(\xi_j) + \underline{\phi}^{(m)}(\xi_j)]. \tag{29}$$

Reaction: For each element, the set of equations

$$\frac{d\phi_\alpha}{dt} = S_\alpha(\underline{\phi}), \quad \alpha = 1,2,3, \qquad (30)$$

is integrated for a time interval Δt, from the initial condition $\phi = \phi^{(n)}(\xi_f, t)$ to produce the new value $\phi^{(n)}(\xi_f, t+\Delta t)$. (In fact, in the computations, reaction is implemented in a more efficient manner, but the effect is that described.)

The analysis of Pope[3] shows that this simulation converges to the solution of Eq. 19, and estimates the truncation error and sampling error caused by a finite number of grid nodes and elements. (The time step Δt was chosen to be very small, $\Delta t = 0.1\, d/U_0$, thus virtually eliminating that source of truncation error.) The calculations were performed with 20 grid nodes (7 of which were in the initial region $\xi \leq 7.5$) and with 25 elements per ensemble (N = 25). Some of the calculations were repeated with 40 grid nodes to check that the truncation error was insignificant. After the steady state had been reached (at $t = 200\, d/U_0$), the calculations were continued with ensemble averages being computed at the end of each of 30 time intervals of duration $10\, d/U_0$. The mean of the ensemble averages was then taken and, according to the analysis of Pope,[3] the result is equivalent to performing the calculations once with N = 750. By this procedure, not only is an accurate result obtained, but also the sampling error can be quantified. The number of time intervals was chosen to be 30 so that the standard sampling error was typically less than 4%. Thus, the calculations reported in the next section are accurate solutions of Eq. 19.

The computations were performed on a VAX 11/780 computer which is about one-tenth the speed of a CDC 7600. The calculations took 2-1/2 minutes CPU time at a cost of $5.00.

Results and Discussion

The Monte Carlo method was used to solve the equation for $\bar{p}(m_{C_3H_8}, m_{CO}, m_{NO}; \xi, t)$ for each of the nine flames studied by Robinson.[1] A comparison of measured and calculated CO concentrations is presented on Fig. 3. These results are for the middle solidity ratio ($s = 0.815$) and the two extreme equivalence ratios ($\phi = 0.635$ and $\phi = 0.845$). The calculations show that the CO concentration rises slightly to a maximum at $\xi \approx 3$ and then decays almost to equilibrium concentrations at $\xi = 60$. The initial rise is caused by the production of CO as propane from the potential cores mixes and reacts. The high diffusivity in the initial region prevents the maximum from being more pronounced. It may be seen that for the weaker mixture ($\phi = 0.635$)

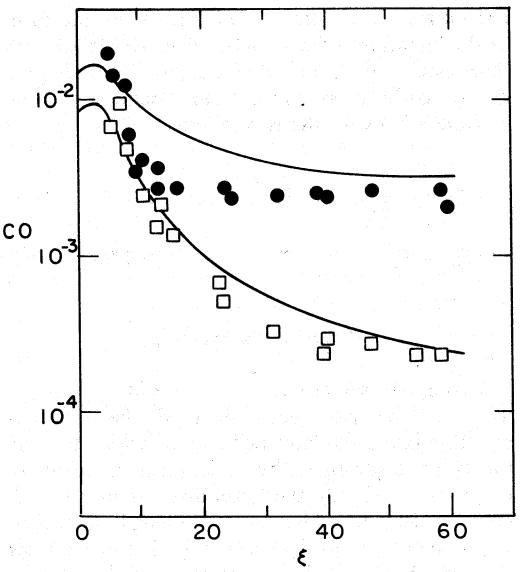

FIG. 3. Mole fraction of CO against axial distance; $s = 0.815$.

● $\phi = 0.845$
□ $\phi = 0.635$
} data of Robinson[1]
—calculations

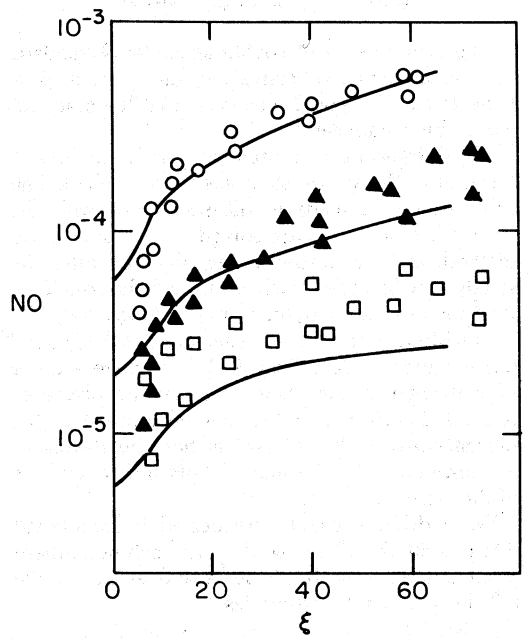

FIG. 4. Mole fraction of NO against axial distance; $s = 0.815$.

○ $\phi = 0.845$
▲ $\phi = 0.725$
□ $\phi = 0.635$
} data of Robinson[1]
—calculations

the agreement between measurements and calculations is very good; for the richer mixture it is apparent that the rate of oxidation of CO is underestimated by the reaction scheme.

The NO concentrations shown on Fig. 4 are for the middle solidity ratio ($s = 0.815$) and all three equivalence ratios. As expected, the NO concentrations rise monotonically with ξ and their levels increase with increasing equivalence ratio. For the highest equivalence ratio ($\phi = 0.845$) the agreement between measurements and calculations is excellent. For the two weaker mixtures the agreement deteriorates slightly as the calculated concentrations fall below the measurements. But, considering the sensitivity of the Zeldovich mechanism to the calculated temperature and 0-atom concentration, this level of agreement is remarkably good.

The calculated mean species concentrations shown on Figs. 3 and 4 were obtained from the Monte Carlo simulation by taking ensemble averages over the elements. The joint *pdf* was recovered from the calculations by forming a histogram from the elements. Figure 5 shows the joint *pdf* of m_{CO} and m_{NO} at $\xi \approx 20$ for $s = 0.815$ and $\phi = 0.635$. Each curve shows $\bar{p}(m_{CO}, m_{NO}; \xi)$ plotted against m_{CO} for a fixed value of m_{NO}. In addition to the curves shown, there is a delta function at ($m_{CO} = 0$, $m_{NO} = 0$) corresponding to inburnt mixture. The magnitude of this delta function (which is the probability of non-zero $m_{C_3H_8}$) is 0.0067.

It is immediately apparent from the figure that CO and NO are negatively correlated. This is to be expected since the effect of reaction is to decrease m_{CO} and to increase m_{NO}. It may also be seen (from the curve at NO = 17 ppm, for example) that $\bar{p}(m_{CO})$ is significantly skewed, with a tail extending to large values of m_{CO}. This tail is yet more evident in the curve for NO = 13 ppm which also shows that the flatness factor is far greater than for a normal distribution. The tails are important since the reaction rates increase rapidly (and non-linearly) with increasing CO. Hence a significant fraction of the reaction can occur in these regions of low probability. Moment formulations—which usually consider

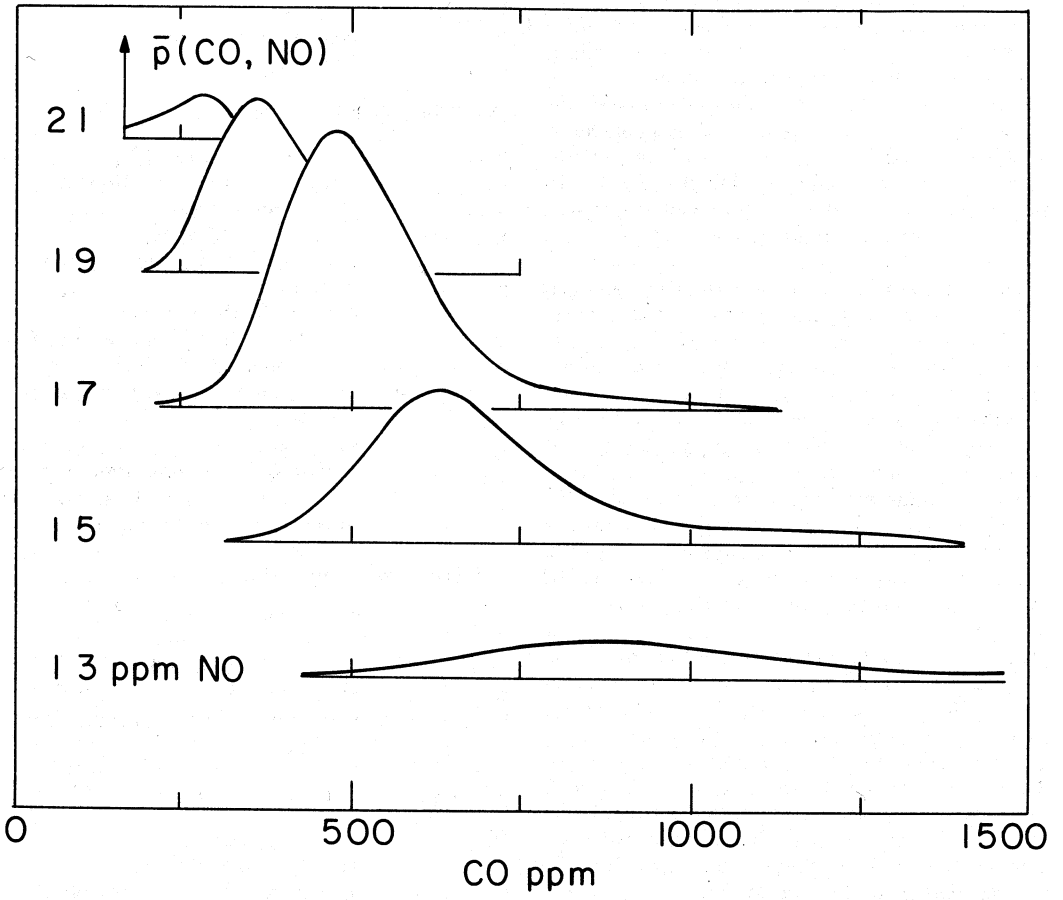

FIG. 5. $\bar{p}(m_{CO}, m_{NO}; \xi = 19.24)$ against CO for NO = 13, 15, 17, 19, 21 ppm; $s = 0.815$, $\phi = 0.635$. (Not shown, probability of $C_3H_8 = 0.0067$.)

only first and second moments—are unlikely to provide accurate descriptions of distributions such as this.

The level of agreement between the present calculations and the data is very encouraging. For the weakest mixture two discrepancies are apparent: these are the underprediction of the NO concentration and the too slow oxidation of CO. A questionable assumption in the reaction scheme is that the number of moles n is uniquely related to m_{CO}. This assumption could be removed by including n as an independent variable. The equation for $\bar{p}(m_{C_3H_8}, m_{CO}, n, m_{NO}; \xi, t)$ could then be solved by the Monte Carlo method. It is likely that this change would decrease if not remove the observed discrepancies.

Conclusion

The Monte Carlo method[3] has been used to solve the transport equation for the joint *pdf* $\bar{p}(m_{C_3H_8}, m_{CO}, m_{NO}; \xi, t)$ for turbulent premixed flames. The calculated concentrations of CO and NO are in good agreement with the measurements of Robinson.[1]

In the reaction scheme it is assumed that the initial oxidation of C_3H_8 to CO proceeds at an infinite rate but that the subsequent oxidation of CO by OH proceeds at a finite rate. This rate of oxidation is determined by a partial equilibrium model in which the mass fraction of CO and the number of moles are constrained by the kinetics. The formation of NO is described by the Zeldovich mechanism with the N-atom concentration assumed to be in the steady state.

The reduction to the single spatial variable ξ is achieved by a simple flow model that introduces a constant β. The value of $\beta = 0.25$ is chosen in order to produce agreement with measured turbulence intensities in non-reacting flow.

With this reaction scheme and flow model, the joint *pdf* equation reduces to an equation for the area-averaged joint *pdf* $\bar{p}(m_{C_3H_8}, m_{CO}, m_{NO}; \xi, t)$. The only parameters and constants involved in the models are standard turbulence model constants and the constant β. The joint *pdf* equation was solved by a Monte Carlo method. On a VAX 11/780 computer this took 2½ minutes CPU time at a cost of $5.00.

In general, the calculated concentrations of CO and NO are in good agreement with the measurements. Figure 4, for example, shows that for the richest mixtures the calculated NO concentrations are in excellent agreement witht the data. The largest discrepancies are for the weakest mixture in which case the rates of formation of NO and oxidation of CO are underestimated. These discrepancies are most likely due to oversimplifications in either the reaction scheme or the flow model.

Above all, this work clearly demonstrates that the Monte Carlo method can be used to solve the joint *pdf* equation for inhomogeneous flows with complex reactions.

Nomenclature

$C_{\epsilon_2}, C_\mu, C_\phi$	turbulence model constants
d	diameter of holes
$E(\underline{\psi})$	mixing term, Eq. 3
$f(\xi)$	mass flux per unit length from potential cores, Eq. 20
k	turbulent kinetic energy
l_c	length of potential cores
m_α	mass fraction of species α
N	number of elements in an ensemble
$n_c, n_1, n_{d\pm}, n_m$	Monte Carlo parameters, Eqs. 25–29
$p(\underline{\psi})$	joint *pdf* of $\underline{\phi}$
$Q(\underline{\phi})$	arbitrary function of $\underline{\phi}$
$S_\alpha(\underline{\phi})$	rate of change of ϕ_α due to chemical reaction
s, s^*	solidity ratio, effective solidity ratio
t	time
U	velocity
u	velocity fluctuation
x	position

Greek Letters

β	model constant, Eq. 13
Γ_T	turbulent diffusion coefficient
δ	Dirac delta function
ϵ	rate of dissipation of k
ξ	normalized axial position, Eq. 6
ρ	density
σ	dimensionality of $\underline{\psi}$-space
σ_ϕ	turbulent Schmidt number, Eq. 4
ϕ	equivalence ratio = (fuel/air ratio)/(stoichiometric fuel/air ratio)
ϕ_α	scalar variable
$\underline{\psi}$	independent composition space variables corresponding to $\underline{\phi}$
ω	turbulent frequency, Eq. 5

Subscripts and Superscripts

i	coordinate direction i
j	finite difference node j
m,n	element of an ensemble
α	scalar variable α
0,1,2	pertaining to upstream, Region I, Region II

Averages

$\langle Q \rangle$	expected value
$\tilde{Q}$	density-weighted mean
$\bar{Q}$	area-averaged, density-weighted mean

$\hat{Q}$	ensemble average
Q''	density-weighted fluctuation
Q^*	departure from $\bar{Q}$

REFERENCES

1. Robinson, G. F.: Pollutant Formation in Turbulent Flames, Ph.D. Thesis, Northwestern University, 1974. (See also, Robinson, G. F. and Kovitz, A.A.: AIAA J *13*, 1488 (1975).)
2. Pope, S. B.: Phil, Trans. R. Soc. Lond. A. *291*, 529 (1979).
3. Pope, S. B.: A Monte Carlo Method for the PDF Equations of Turbulent Flow, M.I.T. Report, MIT-EL 80-012, 1980.
4. Lockwood, F. C. and Naguib, A. S.: Combust. Flame *24*, 109 (1975).
5. Dopazo, C.: Phys, Fluids *18*, 397 (1975).
6. Bray, K. N. C.: Seventeenth Symposium (International) on Combustion, The Combustion Institute, 1979.
7. Janicka, J. Kolbe, W. and Kollmann, W.: J. Nonequilib. Thermodyn. *4*, 47 (1979).
8. O'Brien, E. E.: Statistical Methods in Reacting Turbulent Flows, AIAA 18th Aerospace Sciences Meeting, 1980.
9. Curl, R. L.: A.I.Ch.E.J. *9*, 175 (1963).
10. Launder, B. E. and Spalding, D. B.: Mathematical Models of Turbulence, Academic Press, 1972.
11. Morr, A. R. and Heywood, J. B.: Acta Astronautica *1*, 949 (1974).
12. Jensen, D. E. and Jones, G. A.: Combust. Flame *32*, 1 (1978).
13. Gordon, S. And McBride, B. J.: Computer Program for Calculation of Complex Chemical Equilibrium Compositions, NASA SP 273, 1971.
14. Hill, B. J.: Analysis of Confined Jet Flows with Applications to the Design of Jet Pumps, Ph.D. Thesis, London University, 1971.

COMMENTS

M. Lavid, Exxon Research & Engineering Co., USA. You applied the Monte Carlo method to lean mixtures and obtained good agreement between experimental and calculated data.

My question is, did you or do you plan to apply it to rich mixtures where we expect the NO concentration to reach a minimum? Will your model be also in good agreement with measured concentrations at high equivalence ratios?

Author's Reply. I have not investigated, nor do I plan to investigate, the formation of NO for fuel rich mixtures. I would expect that the modeling of the joint pdf equation would be just as accurate in the fuel rich case, but the chemical kinetics scheme might need improvement.

●

R. W. Bilger, University of Sydney, Australia. I would like to congratulate Prof. Pope on a fine innovative piece of work. I have three questions.

1. In atmospheric pressure flames the water gas shift reaction is usually found to be in equilibrium which implies that the $CO + OH \gtrless CO_2 + H$ reaction is equilibrated as well as the fast shuffle reactions. (The burn-out of CO is then controlled by radical recombination.) In your calculation how close is this reaction to equilibrium? Would you get essentially the same answer if you assumed it was in equilibrium?

2. Your closure for the turbulent convection term involves the gradient flux approximation for reactive scalars. There is an increasing amount of evidence that this modelling is often satisfactory for conserved scalars but is poor for reactive scalars which can even show scalar gradient diffusion. Can your model avoid this difficulty, perhaps by using a perturbation approach?

3. The closure for molecular inter-diffusion is also questionable for reactive scalars. The gradients in the turbulent flame front region of the flow will be determined as much by chemistry as by the large scale turbulence. Can you forsee any way of overcoming this problem?

Author's Reply. In answer to the first question, I do not know how close to equilibrium the CO reaction is. I assumed that it was this reaction that accounted for the above-equilibrium concentrations of CO: but, as you point out, the three-body reactions could be controlling.

In the present calculations, the gradient-diffusion assumption is certainly suspect in the initial region where there are large density differences and rapid reactions. However, since the flame stabilization depends upon the diffusion, and the results are in agreement with the data, the modelling does not appear to be grossly in error. Further downstream, the gradient-diffusion assumption has more foundation but diffusion becomes less important.

In an extension of the present model, the gradient-diffusion is completely avoided. Instead of solving

for the pdf of scalars, the equation for the joint pdf of velocity and scalars can be solved by the Monte Carlo method. Not only is the gradient-diffusion assumption avoided in this approach, but a turbulence model to determine the Reynolds stresses is no longer required.

The present modelling of the molecular mixing term is indeed suspect when reaction as well as turbulence is responsible for intensifying the scalar gradients. In the present calculations, downstream of the stabilization zone, the mixing is most likely controlled by the turbulence, and so the modelling may be satisfactory. The problem of determining scalar dissipation rates is a difficult one, even in non-reacting flows. It may be that two-point closures will be needed to guide the way to modelling at the one-point level.

●

R. Maly, University of Stuttgart, West Germany. Could you comment on computing times when more species or other processes (e.g. heat loss to walls) or more nodes are included?

Author's Reply. To a first approximation, the number of computer operations required by the Monte Carlo method is linearly proportional to the product of the number of grid nodes and the number of scalars (species and enthalphy). In the present application, the system is adiabatic and so the enthalpy is constant. If, however, heat loss were important, the enthalpy could be added to the set of scalars. The amount of computer time would then rise by one third.